

GLOBAL JOURNAL OF ENGINEERING SCIENCE AND RESEARCHES

EVALUATION OF STRESSES IN DIFFERENT CONFIGURATION OF NOTCHED GEOMETRY USING FINITE ELEMENT SIMULATION

R. D. Palhade

Professor, Department of Mechanical Engineering, Anuradha Engineering College, Chikhli, Dist-Buldhana, (MS), India-443201

ABSTRACT

Various shapes of notches are widely used by designers in order to optimize the shape of the engineering components and structures. These notches are the most susceptible case for fracture in parts. The optimization of machine element forces, constructors to design complex elements that have to meet strength requirements. Geometry of these elements favours to various stresses under variable service loading which may cause machine destruction. The value of the stress and strain may exceed permissible limits at the notch tip. Since notch is unavoidable part of many engineering components and structures, it becomes necessary to analyse and correlate different notch geometries to specify the least vulnerable notch geometry. In this study compares the different notch geometries in axial loading condition on the basis of maximum principle stress. The numerical and experimental investigations were used to evaluate the stress values for different notches.

Keywords: Notch configuration, Finite element simulation, Photo-elasticity, Principle stresses.

I. INTRODUCTION

High local stresses may cause a local damage to notched structures under static or variable loading, and greatly affect the load-bearing capacity of the structures. Thus, a good understanding of stresses in the vicinity of the notch tip and the ability to predict the initiation of fracture are of fundamental importance for a reliable failure analysis of engineering components and structures containing notches. In order to evaluate the validity of PS and MS criteria, the theoretical values of compressive notch fracture toughness were compared with the experimental results [1]. The results showed that while the MS model with a total difference of 5% was an appropriate failure criterion whereas the PS model with about 86% accuracy could not predict the experimental results satisfactorily. An application of the mode II Generalised Notch Stress Intensity Factor (NSIFs) for U shaped and V-shaped radius notches, varying the notch radius as well as the notch opening angle studied by [2]. It was observed, when the notch radius tends to zero the mode II Generalised NSIF does not converge to the NSIF as defined for pointed V-notches and the discrepancies between the two parameters strongly depend on the notch shape. An analytical expression for the Stress Intensity Factor (SIF) related to a crack emanating from a root of blunted V notch was reported [3]. Different notch amplitudes (ranging from 0° to 180°) and different crack length to root radius ratios (ranging from 0 to 10) were taken into account. The proposed formula significantly improved the predictions of the relationships available in the literature, by considering notch amplitude as a dependent parameter. In this case applied microstructure fracture mechanics and numerical techniques to study the fatigue limit of components with notches of arbitrary form subjected to mode I loading [4]. Comparisons with experimental results on specimens with different flange angles, root radii and notch depths were reported. Formulae for stress concentration factor with more than 1% accuracy using Neuber formula and the solution of a V-notch in a semi-infinite plate was proposed by [5]. Designed and optimised double edge notch tension compression specimen using linear elastic fracture analysis. The specimen geometry allows the user to efficiently obtain fatigue crack growth data under displacement controlled test with least load misalignment [6]. A 2-D finite element and boundary element analysis were used to obtain stress-intensity factors and displacements over a wide range in crack-length to width ratios. This investigation reveals a height to width ratio of at least 1.2 was required to ensure that the stress intensity and displacements were not highly dependent on the gage length. [7] Analysed the stresses on inter vertebral disc between vertebrae L4 and L5 when a compressive load was applied on vertebra L4 using the photoelasticity transmission technique and the finite element method. Simulation was carried out using a load of 23N. The analysis showed that the stress generated by the vertebrae on inter vertebral disc was higher in the poster lateral region. The method of photoelasticity to study the

effects of first non-singular stress term on isochromatic fringe patterns around the tip of a mode I sharp V-notch accessed [8]. Notches were divided into two categories i.e. notches with opening angles a) less than 45° , b) between 45° and 152° . Using this specimen, different loading conditions were simulated by changing the lateral load ratio and consequently different effects of the first non-singular term on the shape and size of the fringes were investigated experimentally. Good correlation between the analytical and experimental results was observed. They Calculated NSIFs for a laboratory specimen called V-notched Brazilian disk for various notch angles under pure mode I, pure mode II and mixed mode I/II loading conditions [9]. In addition to NSIFs, the coefficient of the first non-singular term of 30° notch was calculated experimentally and the effects of this term on the stress distribution in the vicinity of notch tip were investigated. A good correlation was observed between the experimental results and the numerical results obtained from finite element analysis. [10] Performed fatigue experiments on single edge notch specimens of EN AW 7475-T761 in order to investigate cyclic lifetime changes due to sharp notches and periodic overloads. They observed that on the fracture surfaces a decrease in the crack propagation rate to a certain distance which was followed by an increase of the crack propagation rate till fracture. Thus, they concluded that different distances to the minima of the crack propagating rate depend on the type and the level of the periodic overload as well as on the notch depth. In another study conducted a series of experiments on gas turbine blade like specimens. The specimens were impacted with a cubical projectile at 250 m/s using a gas gun. They were subsequently fatigue loaded using the step method of testing to establish the fatigue strength in the damaged state [11]. The effects of impact angle, leading edge radius, and blade wedge angle were investigated. It was shown that damage depth has a significant effect on fatigue strength. [12] Proposed strain gage method for experimental determination were verified with theoretical results of SIF of sharp notched strips in mixed loading. In this paper performed an experimental and numerical study to ascertain the influence of V-notches on the strength of different brittle materials [13]. In addition to this, the influences of the V-notch angle, V-notch depth as well as the influence of specimen size and type of loading were determined by testing three-point bend beams and single edge notch tensile specimens. Above discussion shows more work is done on analysing stresses parameters for V Notch. No remarkable illustrations are available on other notch geometries. Hence in present research work is carried out and discussed by using experimentally and numerically to correlate other notch geometries i.e. square and semi-circular notch, with sharp V notch on the basis on maximum principle stresses to find out the most suitable notch geometry for the engineering components or structures.

II. EXPERIMENTAL INVESTIGATION

In this study photo-elasticity is selected as an experimental method for stress analysis. The response variable selected to achieve different values of maximum principle stress are three different configurations of notches in axial loading conditions. Parameters used in the investigation are notch depth, notch area, applied load and maximum principle stress. The experiments were conducted using whole field method of stress analysis.

2.1.

2.2. Selection of material and preparation of test specimens

Epoxy resin is selected for the present study because of its high photo-elastic sensitivity and high degree of freedom from mechanical and optical creep. Epoxy resins are easily machinable and have little time-edge effect. Time-edge effect causes compressive stresses at the edges of the model passing with time. The most commonly used photo elastic model material for two dimensional photoelastic analyses is cold setting epoxy resin. The mechanical properties of the selected epoxy resin CY – 230 and hardener HY – 951 are given in Table 1.

Table 1. Mechanical properties of epoxy resin

Name	Trade Name	Young's Modulus (MPa)	Poisson's ratio
Epoxy resin	Araldite CY 230 and 10 % Hardener HY- 951	2570.22	0.38

First of all the mould surface is thoroughly cleaned using cloth followed by mould is levelled on the table. The mould surface is then coated with mould release agent silicon spray. The hardener is added in the resin 10 % by weight for proper casting. These two materials are mixed in a glass beaker slowly using a stirring rod to yield a homogeneous mixture without exhibiting streaks of hardener in the mixture. The care has been taken to see that air

[NC-Rase 18]

DOI: 10.5281/zenodo.1493996

ISSN 2348 – 8034

Impact Factor- 5.070

bubbles are not entrapped in the mixture. The mixture is then poured into the mould. The setting time for the sheet is 18-24 hours or more, depending upon the quantity of the mixture and the shape of the mould. After setting the casting is removed from the mould. It is next kept on a flat surface for curing. Normally, periods of at least ten days are required for completion of a polymerization process. Now the casting is ready for preparation of two dimensional photoelastic models. Then the calibrations of these prepared samples are carried out by using following procedure. A circular disc of 60 mm in diameter is cut out of the same sheet. The disc is loaded under the diametrical compression on circular polariscope. The load is increased gradually. The fringe order at the centre of the disc and corresponding load are recorded. The material fringe value is calculated using the Eqs.1.

$$F_{\sigma} = \frac{8P}{\pi DN} \quad (1)$$

Where, P is the load (N),

D is the diameter of the circular disc (mm),

N is the fringe order.

2.2 Preparation of model template

The specimen models were cut from a casted sheet. To cut the models from sheet a standard procedure is followed. If more than 2 or 3 pieces of the same shape are to be made, it is advisable to machine a template cut of metal first. This template may then be used to fabricate multiple photo-elastic specimens having the same shape as that of the template. The template should be undercut by about 1-2 mm through about half the template thickness from one side to avoid contact with the router bit. Then a band saw blade with a sharp, narrow is used to rough cut the shape of the specimen. A generous allowance of about 3 mm should be marked on the specimen all around the template edge, since the blade will heat the material and nick the edge. Then a router with a high-speed carbide router bit, preferably with fine multiple flutes, should be used to fabricate the edge of the model. Succession of two centering pins, the first having a diameter larger than that of the router bit, and the second one the same size should be used so that excess material can first be removed quickly and then in a very controlled manner, leaving the specimen with the same dimensions as those of the template.

If the specimen has holes, such as those used for load-application points using pins, then these holes should be drilled carefully with a sharp bit with plenty of coolant, such as ethyl alcohol, kerosene, or water; otherwise unwanted fringes will develop around the edge of the hole. Following are the specimen of sharp V, square and semi-circular notches of different area and depth, which were taken for the experimentation. The dimensions of the specimen are 200 mm in length, 50 mm in width and 5 mm in thickness as shown in Figure 1.

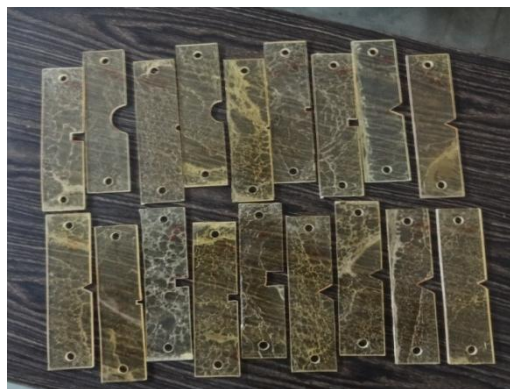


Figure 1. Specimens of different configurations

2.3 Experimental procedure

In order to carry out principle stress by photo-elastic experimental analysis, the notched specimen is fixed in the loading equipment. The polariscope is arranged to get a dark field. The model is stressed in tension using hydraulic pump attached to the setup. Now, fringes are seen in the model, and are counted, beginning from the outermost fringe and ending with the innermost. This gives the integral fringe order. Fractional fringe order is measured by

[NC-Rase 18]

DOI: 10.5281/zenodo.1493996

ISSN 2348 – 8034

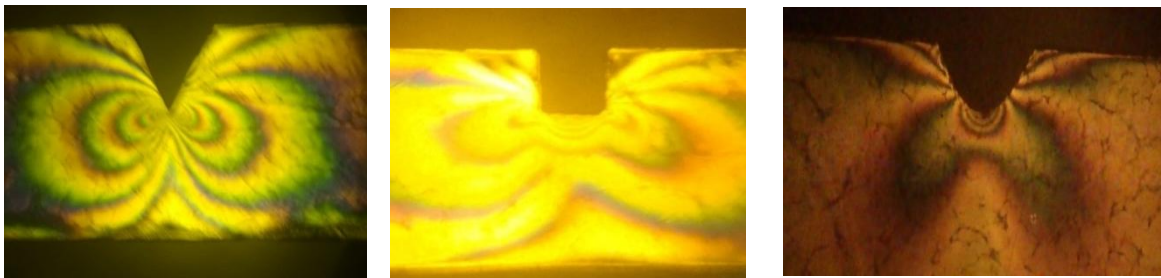
Impact Factor- 5.070

rotating the analyzer such that the fringe of interest passé through the center of the specimen. Total fringe order is then calculated. Knowing material fringe constant and fringe order, the maximum stress near the notch is calculated. Then the determination of isochromatic fringe order at a point is carried out. When model is loaded in polariscope due to the property of birefringence fringes are produced in the model. To determine the stress level at that particular load fringe order (N) is needed. In order to determine isochromatic fringe order at a point, the polariscope is set to dark field arrangement and white light or mono-chromatic light is used. The fringe order can be determined in terms of complete fringe order or fractional fringe order.

When white light is used in circular polariscope, isochromatic fringes appear colored. These coloured fringes are determined in terms of fractional fringe order. Fractional fringe order is generally found in the cases where the highest fringe order is low the integral and half order fringe estimate in the region of the interest not sufficient. Hence fringe colour sequence provided by [14] is used to identify the fringe order. Here, fractional fringe order was observed only for uniform specimen i.e. specimen without notch. These colour sequence is observed in the model when stressed in incremental manner. Fig 2 shows the fringe pattern for specimen without notch in axial loading condition at 1000 N of load. Initially, black colour was observed over the entire field of unstressed specimen. As the model is stressed, colored fringes are observed in the same sequence as stated. The highest order colour observed in the model is green-yellow after the first tint of passage. Hence, the fringe order is 1.39. When monochromatic light is used in circular polariscope, complete fringe order isochromatic fringes are observed. Figure 3 (a), (b) and (c) show the fringe pattern for notched specimen with area of 200 mm² and 15 mm depth respectively. Fringe order for sharp V, square and semi-circular notch at 200 mm² of area are 10, 6 and 6 respectively and fringe order for sharp V, square and semi-circular notch at depth 15 mm are 7, 7 and 7 respectively.



Figure 2. Isochromatic fringe pattern for un-notched specimen at 1000 N of load



(a) Sharp V notch

(b) Square Notch

(c) Semi-circular Notch

Figure 3. Isochromatic fringe pattern for sharp V, square and semi-circular notch at 200 mm² of area

2.3 Calculation of maximum principle stress

The observed fringe order provides immediate qualitative information about the maximum principle stress; stress concentrations and some other stress parameters using the principle of stress optic law are as given in Eqn. (2).

$$\sigma_1 - \sigma_2 = \frac{Nf_\sigma}{h} \quad (2)$$

Where, σ_1 and σ_2 are maximum and minimum principle stresses at the point (MPa),

N is the fringe order,

f_σ is the material fringe value (N/mm),

h is the thickness of the specimen (mm).

Hence, the maximum principle stress at any point in case of uniaxial tension specimen, where $\sigma_2 = 0$, can be stated as

$$\sigma_1 = \frac{Nf_\sigma}{h} \quad (3)$$

Using Eqn. (3) the value of maximum principle stress for any fringe order is calculated.

III. FINITE ELEMENT SIMULATION OF NOTCHES

In present stress analysis using finite element simulation in order to find out stresses and its effects, for varying depth and area of notch are considered for three different cases as sharp V, square and semi-circular notch. A schematic diagram of the thin rectangular plate specimen with sharp V, square and semi-circular notch geometries are shown in Figures 4 (a), (b) and (c) respectively. The geometric characteristics of the specimen were considered same as experimental case. For Sharp V-notch, the flange angle (α) was kept fixed at angle 60° . In this paper commercially available FE software AnsysTM-15 is used for the 2-D stress-strain calculations. The test specimen model is generated with the help of key points later joined by straight lines and then forming 2D area model. It involves generation of a rectangle of size 200 mm \times 50 mm and 5 mm of thickness. Thickness can be given by extrusion operation or by adding thickness to real constants. To create the sharp V notch, square and semi-circular notch in the specimen 'Subtract areas' option is used.

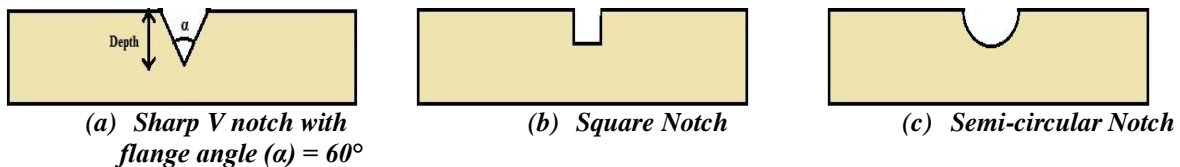


Figure 4. Thin rectangular plate specimen with different geometry

The element plane-183 is found the best suitable element for this type of geometry as well as for present structural analysis in AnsysTM15 program. The Plane-183 element consists of the following characteristics. The element can be used as either a plane element (plane stress, plane strain or generalized plane strain) or an axisymmetric element. It is defined by four nodes having two degrees of freedom at each node: translations in the nodal x and y directions as shown in Figure 5. The element has plasticity, hyperelasticity, stress stiffening, large deflection, and large strain capabilities.

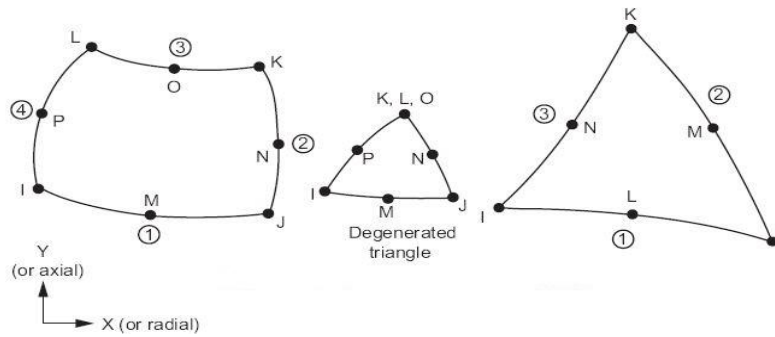


Figure 5. Geometry and node locations for Plane-183

Adding material properties to the modeled specimen is done by using ‘Material Models’ option which is available in the ‘Material Props’. The material properties of the selected epoxy resin are given in Table 1. Then an axial force of magnitude 500 N and 1000 N are applied for the present static FE simulation. The force is applied on right side edge-line all nodes of test specimen, while the left side edge-line all nodes are considered fixed as a zero degree of freedom as shown in Figure 6 Finally, the structural static finite element analysis is performed.

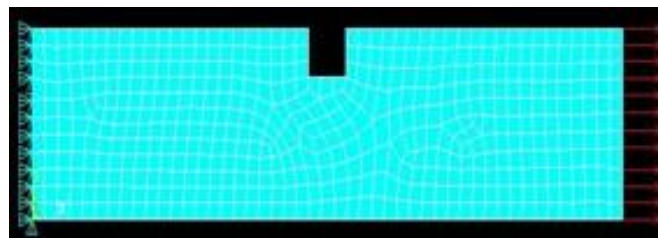


Figure 6. Test Specimen with square notch and its loading condition

After application of loading and boundary condition, ‘Solve’ option is used to obtain the solution. Solution for maximum principle stress is available in ‘Nodal Solu’ option. The result for unnotched specimen, sharp V notch for the area of 200 mm² and depth of 15 mm are shown in Figures 7, 8 and 9, respectively only here

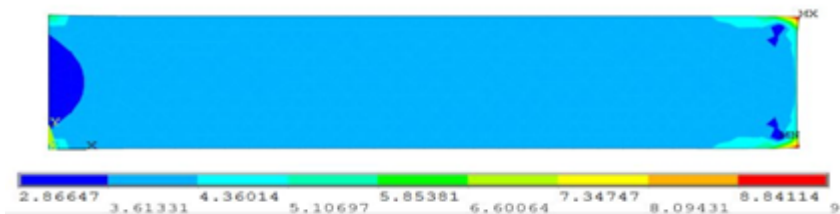


Figure 7. Maximum principle stresses for un-notched specimen

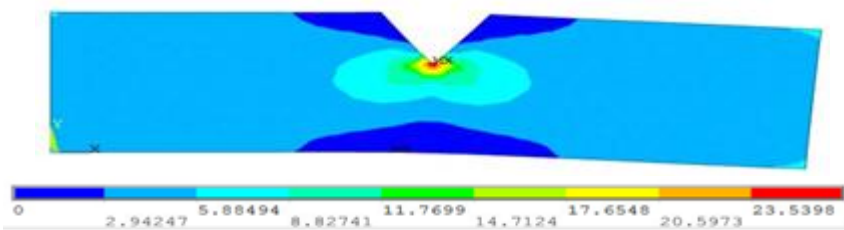


Figure 8. Maximum principle stresses for sharp V notch specimen for the area of 200 mm²

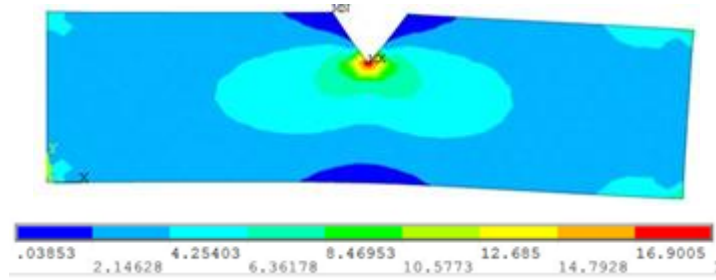


Figure 9. Maximum principle stresses for sharp V notch specimen for the depth of 15 mm

IV. RESULT AND DISCUSSION

Experimental Photo-elastic method and finite element simulation were used to investigate the maximum principle stress for different notch configurations at various load levels in the present work. The comparisons of photo-elasticity and finite element simulation results are presented in following sections for different area and depth. The results obtained from numerical analysis shows good agreement with the experimental results.

The results for maximum principle stress for sharp V, square and semi-circular notches are executed. The readings were taken for notched and un-notched specimens in axial loading condition with magnitude 250 N, 500 N, 750 N and 1000 N. Scales for notch area and depth were considered for notch geometries in the range of 50-200 mm² and 5-20 mm respectively as a variable parameter for these analyses. The dimensions of the specimen were considered as 200 mm in length, 50 mm in width and 5 mm in thickness. Figure 10 and 11 shows the comparison between experimental and numerical result for sharp V notch, varying area and depth respectively.

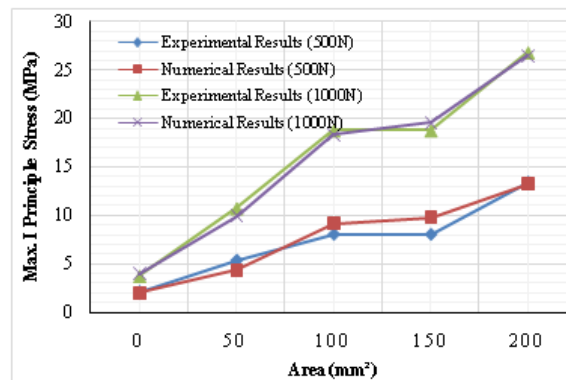


Figure 10. Comparison of experimental results and numerical results for sharp V notch for varying area

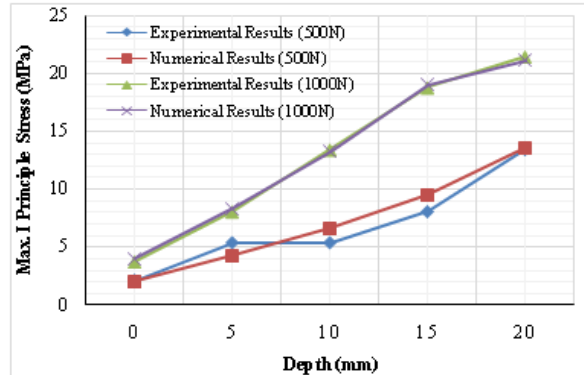


Figure 11. Comparison of experimental results and numerical results for sharp V notch for varying depth

Figure 12 and 13 shows the comparison between experimental and numerical results for square notch for varying area and depth respectively.

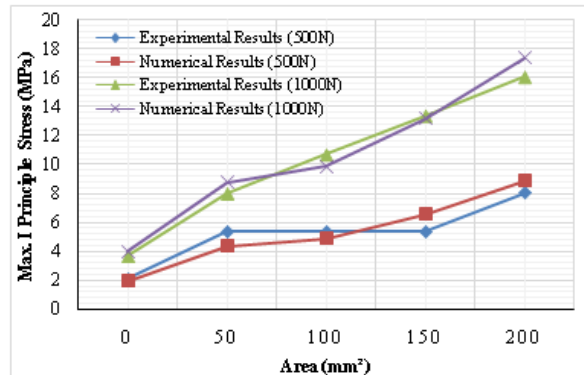


Figure 12. Comparison of experimental results and numerical results for square notch for varying area

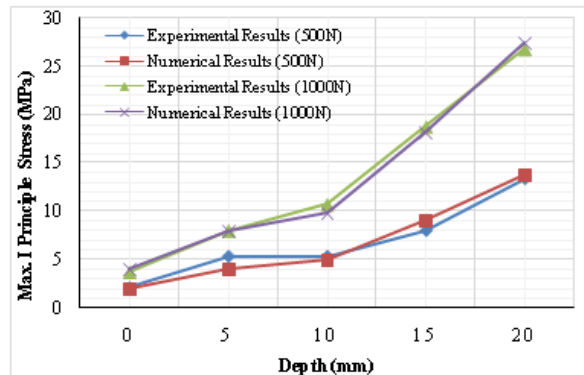


Figure 13. Comparison of experimental results and numerical results for square notch for varying depth

Figure 14 and 15 shows the comparison between experimental and numerical results for semi-circular notch for varying area and depth respectively. These figures also portray the experimental and numerical results in good agreement with each other.

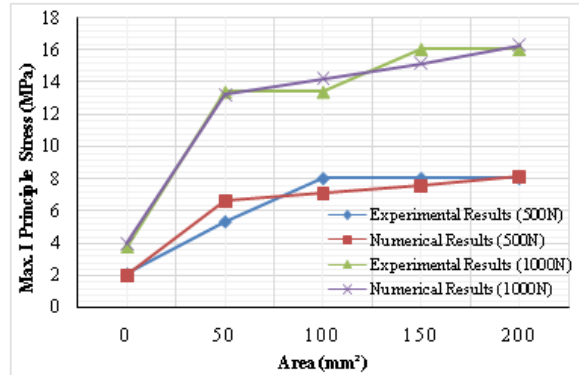


Figure 14. Comparison of experimental results and numerical results for semi-circular notch for varying area

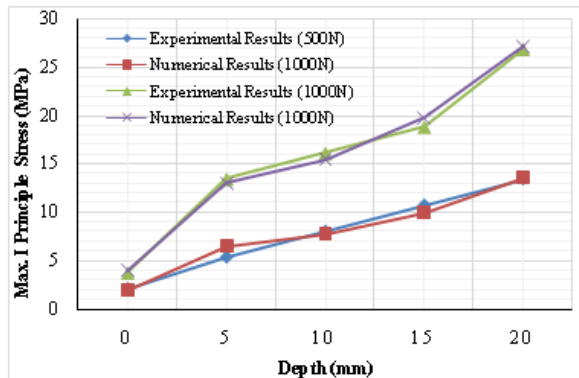


Figure 15. Comparison of experimental results and numerical results for semi-circular notch for varying depth

The Table 2 and 3 shows comparison of experimental and numerical results for sharp V, square and semi-circular notch for varying area and depth respectively.

It is observed from Figures 10, 12, 14 and Table 2 that the maximum principle stress for notch geometry increases with the increase in the area of the notch. Whereas sharp V notch shows a steep rise in maximum principle stress as compared to other notch geometries. The steep rise in maximum principle stress of sharp V notch is because, when the area of sharp V, square and semi-circular notch are kept constant, the relative rise in the depth of sharp V notch is much more than square and semi-circular notch. Same is observed in case of increase in depth of these notch geometries. It is more clearly illustrated from Figures 11, 13, 15 and Table 3 that the maximum principle stress for notch geometry increases with the increase in the depth of the notch. Whereas semi-circular and square notch shows a steep rise in maximum principle stress as compared to sharp V notch. The steep rise in maximum principle stress of semi-circular and square notch is because, when the depth of sharp V, square and semi-circular notch are kept constant, the relative rise in the area of semi-circular and square notch are much more than sharp V notch.

Table 2. Comparison of experimental (E) and numerical (N) results for sharp V, square and semicircular notch for varying areas

Area (mm²)	Load (N)	Maximum I Principle Stress (MPa)					
		Sharp V Notch		Square Notch		Semi-circular Notch	
		E Results	N Results	E Results	N Results	E Results	N Results
0	500	2.12	2.00	2.12	2.00	2.12	2.00
	1000	3.72	4.00	3.72	4.00	3.72	4.00
50	500	5.36	4.38	5.36	4.38	5.36	6.62
	1000	10.73	9.97	8.04	8.76	13.41	13.25

100	500	8.04	9.15	5.36	4.94	8.04	7.14
	1000	18.77	18.31	10.73	9.88	13.41	14.27
150	500	8.04	9.80	5.36	6.58	8.04	7.61
	1000	18.77	19.61	13.41	13.17	16.09	15.20
200	500	13.41	13.24	8.04	8.91	8.04	8.16
	1000	26.82	26.48	16.09	17.38	16.09	16.32

Table 3. Comparison of experimental (E) and numerical (N) results for sharp V, square and semicircular notch for varying depth

Depth (mm)	Load (N)	Maximum I Principle Stress (MPa)					
		Sharp V Notch		Square Notch		Semi-circular Notch	
		E Results	N Results	E Results	N Results	E Results	N Results
0	500	2.12	2.002	2.12	2.00	2.12	2.00
	1000	3.72	4.005	3.72	4.00	3.72	4.00
5	500	5.36	4.184	5.36	4.31	5.36	6.49
	1000	8.04	8.368	8.04	8.00	13.41	13.10
10	500	5.36	6.618	5.36	4.94	8.04	7.72
	1000	13.41	13.23	10.73	9.88	16.09	15.44
15	500	8.04	9.50	8.04	9.10	10.73	9.91
	1000	18.77	19.01	18.77	18.21	18.77	19.81
20	500	13.41	13.56	13.41	13.73	13.41	13.57
	1000	21.46	21.12	26.82	27.47	26.82	27.14

It is observed that a single notch results in a high degree of stress concentration. The severity of stress concentration is reduced by the use of multiple notches. In this case, the sharp bending of a flow force line is reduced and it follows a smooth curve. The notch amplitude may be dependent parameter, as long as the crack length is sufficiently small with respect to the notch depth. It is further reveal that there exists a strong influence of the gage length on the stress intensity and the displacements. A height to width ratio of at least in range 1.2 to 1.3 was required to ensure that the stress intensity and displacements were not highly dependent on the gage length. It shows that on the fracture surfaces a decrease in the crack propagation rate to a certain distance which was followed by an increase of the crack propagation rate till fracture. It may be due to distances to the minima of the crack propagating rate depends on the type and the level of the periodic overload as well as on the notch depth. The notch strength are influenced by notch angle in case of V-notch, notch depth, specimen size, type of loading as well as material types.

V. CONCLUSIONS

Maximum principle stresses were experimentally and numerically determined for various configurations of notched specimens. Stress analysis was performed on epoxy material specimens with sharp V, square and semi-circular notch in axial loading conditions. Notch area and depth were considered as a varying parameter to check their effect on the maximum principle stresses. Thus, the following observations were made from the present investigations:

- Maximum principle stress of the notched component increases with the increase in depth or area of the notch.
- Semi-circular notch is the least vulnerable notch geometry when the requirement of notch area is more. The magnitude of maximum principle stress for semi-circular notch is 16.32 MPa as compared to sharp V notch 26.482 MPa at 200 mm² of area.
- Sharp V notch is the least vulnerable notch geometry when the requirement of notch depth is more. The magnitude of maximum principle stress for Sharp V Notch is 21.127 MPa as compared to semi-circular notch 26.482 MPa at 20 mm of depth.
- Thus from the above observation it is concluded that semi-circular notch is found to be most suited notch geometry during shape optimization of the engineering component.

- These computer simulation results were compared with experimental results and available literature, which shows 3 to 6 % variation in principle stress results. The computer simulation results obtained using finite element method software, thus can avoid costly and time consuming experimental setups.

VI. ACKNOWLEDGEMENT

The author wish to acknowledge the help received from Mr. Gaurav Agarwal PG scholar and Mr. V. S. Bharate, Lab. Assistant, Department of Mechanical Engineering, SSGMCE, Shegaon-444203 for conducting the experiments

REFERENCES

1. A.R. Torabi, M.R. Ayatollahi, "Compressive brittle fracture in V-notches with end holes", *European Journal of Mechanics A/Solids* 45, (2014), pp. 32-40.
2. Alberto Saporita, Pietro Cornetti, and Alberto Carpinteri, "Analytical Stress Intensity Factors for Cracks at blunted V-notches", *Procedia Materials Science* 3, (2014), pp. 738 – 743.
3. D. Nowell, P. Duo and I.F. Stewart, "Prediction of fatigue performance in gas turbine blades after foreign object damage", *International Journal of Fatigue* 25, (2003), pp. 963–969.
4. Dominic Tiedemann, Jürgen Bär and Hans-Joachim Gudladt, "The crack propagation rate according to notches and overload levels", *Procedia Materials Science* 3, (2014), pp. 1359 – 1364.
5. F. J. Gomez and M. Elices, "Fracture of components with V-shaped notches, *Engineering Fracture Mechanics*, 70, (2003), pp. 1913-1927.
6. M. Zappalorto, P. Lazzarin, F. Berto, "Notch Stress Intensity Factors Applied to U and V-Shaped Radiused Notches under In-plane Shear Loading", *Procedia Engineering* 10, (2011), pp. 1115–1120.
7. M. R. Ayatollahi, M. Dehghany and M.M. Mirsayar, "A comprehensive photoelastic study for mode I sharp V-notches", *European Journal of Mechanics A/Solids* 37, (2013), pp. 216-230.
8. M. R. Ayatollahi and M. Nejati, "Experimental evaluation of stress field around the sharp notches using Photoelasticity", *Materials and Design* 32, (2011), pp. 561–569.
9. N. A. Noda, M. Sera, and Y. Takase, "Stress concentration factors for round and flat test Specimen with notches", *International Journal of Fatigue* 17, (1995), pp. 163–178.
10. S. B. Narasimhachary, A. Saxena, and J.C. Newman Jr., "A double edge notch specimen design for tension–compression fatigue crack growth testing", *Engineering Fracture Mechanics* 92, (2012), pp. 126–136.
11. Sarah Fakhri Fakhouri and Suraya Gomes Novais-Shimano, "Photoelastic and Finite Element Stress Analysis of the Gap between the L4 and L5 Vertebrae", *ISRN Mechanical Engineering* (2011).
12. T. Kondo, M. Kobayashi and H. Sekine, "Strain Gage Method for Determining Stress Intensity of Sharp-Notched Strips", *Experimental Mechanics* (2000).
13. V. Chaves and A. Navarro, "Fatigue limits for notches of arbitrary profile", *International Journal of Fatigue* 48, (2013), pp. 68–79.
14. K. Ramesh, "Digital Photoelasticity Advanced Techniques and Applications", Springer Berlin Heidelberg (2000).